J|A|C|S
ARTICLES
Published on Web 11/18/2005

Solution ^{1}H NMR Confirmation of Folding in Short *o*-Phenylene Ethynylene Oligomers

Ticora V. Jones,[†] Morris M. Slutsky,[†] Roberto Laos,[‡] Tom F. A. de Greef,[§] and Gregory N. Tew*,[†]

Contribution from Polymer Science & Engineering, University of Massachusetts, Amherst, Massachusetts 01003, Chemistry Department, University of Florida, Gainesville, Florida 32611, and Materials Technology, Eindhoven University of Technology, 5600 MB Eindhoven, The Netherlands

Received May 30, 2005; Revised Manuscript Received September 27, 2005; E-mail: tew@mail.pse.umass.edu

Abstract: Oligomers based on an *o*-phenylene ethynylene (oPE) backbone with polar substituents have been synthesized using Sonogashira methods. Folding of these extremely short oligomers was confirmed via 1D and 2D (NOESY) NMR methods. Utilizing electron-rich and electron-poor phenylene building blocks, variations of these oPE oligomers have been synthesized to determine the folded stability of π-rich vs π-poor vs π-rich$-\pi$-poor systems. Slight variations in temperature offer a route, aside from solvent denaturation, to probe the stability of the folded structure. This is the first report of an NMR solution characterization of folding for a PE backbone without hydrogen bonds.

Introduction

Foldamers have attracted great interest because of their implications and similarity to folded proteins.[1] Solvent, temperature, metal−ligand interactions,[2] electrostatic differences,[3] hydrogen bonding,[4] and structurally rigid design elements have all promoted folding. These various interactions have been studied for a wide variety of structures from those with biological origin such as β and other peptides,[5] peptoids,[6] saccharides,[7] and nucleic acids[8] to those that lack any biological construct but similarly form helical, extended, and/or turned structures.

Here we report the 1D and 2D solution NMR characterization of new *o*-phenylene ethynylene (oPE) oligomers containing polar triethylene glycol monomethyl ether (Teg) side chains. NMR characterization shows that even the short tetrameric oligomers of this backbone, shown in Figure 1, are capable of folding. Previous work with *m*-phenylene ethynylenes (mPEs) created systems that fold into pucklike helices upon solvent change.[9]

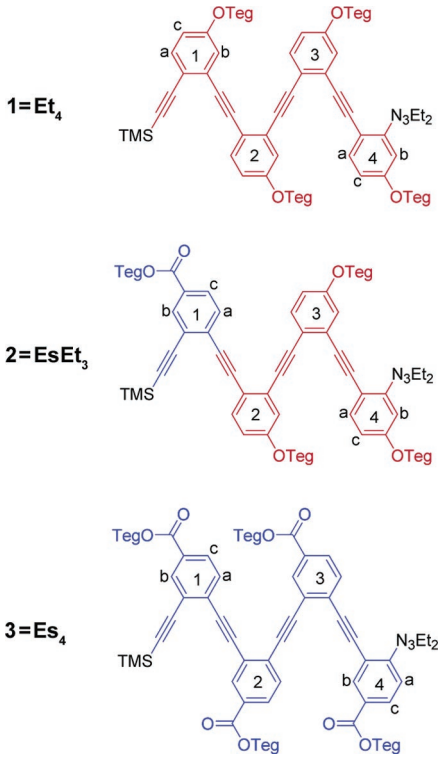

Figure 1. oPE tetramers **1**−**3**. Electron-rich (red) and electron-poor (blue) rings are shown. Relevant protons for each tetramer are labeled. Each ring of each oligomer has three protons that are labeled with respect to their *J*-coupling and splitting pattern, respectively: a (8.4 Hz, d), b (2.1 Hz, d), and c (8.4 and 2.1 Hz, dd).

[†] University of Massachusetts.
[‡] University of Florida.
[§] Eindhoven University of Technology.

(1) (a) Cheng, R. P. *Curr. Opin. Struct. Biol.* **2004**, *14*, 512−520. (b) Gellman, S. H. *Acc. Chem. Res.* **1998**, *31*, 173−180.; (c) Hill, D. J.; Mio, M. J.; Prince, R. B.; Hughes, T. S.; Moore, J. S. *Chem. Rev.* **2001**, *101*, 3893−4011.
(2) Stadler, A. M.; Kyritsakas, N.; Lehn, J. M. *Chem. Commun.* **2004**, 2024−2025.
(3) Nguyen, J. Q.; Iverson, B. L. *J. Am. Chem. Soc.* **1999**, *121*, 2639−2640.
(4) Gong, B.; Zeng, H. Q.; Zhu, J.; Yuan, L. H.; Han, Y. H.; Cheng, S. Z.; Furukawa, M.; Parra, R. D.; Kovalevsky, A. Y.; Mills, J. L.; Skrzypczak-Jankun, E.; Martinovic, S.; Smith, R. D.; Zheng, C.; Szyperski, T.; Zeng, X. C. *Proc. Natl. Acad. Sci. U.S.A.* **2002**, *99*, 11583−11588.
(5) Cheng, R. P.; Gellman, S. H.; DeGrado, W. F. *Chem. Rev.* **2001**, *101*, 3219.
(6) Wu, C. W.; Sanborn, T. J.; Huang, K.; Zuckermann, R. N.; Barron, A. E. *J. Am. Chem. Soc.* **2001**, *123*, 6778−6784.
(7) Chakraborty, T. K.; Ghosh, S.; Jayaprakash, S.; Sharma, J.; Ravikanth, V.; Diwan, P. V.; Nagaraj, R.; Kunwar, A. C. *J. Org. Chem.* **2000**, *65*, 6441
(8) Vilaivan, T.; Suparpprom, C.; Harnyuttanakorn, P.; Lowe, G. *Tetrahedron Lett.* **2001**, *42*, 5533−5536.
(9) Nelson, J. C.; Saven, J. G.; Moore, J. S.; Wolynes, P. G. *Science* **1997**, *277*, 1793−1796.

This system has been characterized using a variety of methods including electron paramagnetic resonance (EPR),[10] circular dichroism (CD),[11] and fluorescence.[12a,b] Despite these extensive investigations, 2D solution NMR characterization of folded PE structures, without extensive hydrogen bonds,[4] has not been reported.

In comparison to mPE oligomers, few oPE sequences have been synthesized,[12c−e] and no folding systems have been reported thus far. Computational and simple torsional considerations suggest that the oPE oligomers have a high probability of folding even with very short sequences.[13] Moreover, the aspect ratios for folded mPE and oPE oligomers are considerably different, leading to distinct geometric shapes. For example, dodecamers of mPE and oPE would form pucks and tall cylinders, respectively. Therefore, the ability to create oPE sequences that fold is being explored, and this is our initial report that confirms folding in these systems.

Results and Discussion

The oPE oligomers reported here were synthesized using standard Sonogashira methods reported earlier[12d] in good yield to afford three tetramers of different electronic compositions. The oligomers shown in Figure 1 include an electron-rich tetramer, **1** (Et_4), where all of the Teg side chains are attached to the oPE backbone through ethers, a mixed system, **2** ($EsEt_3$), with one electron-poor ester ring and three electron-rich ether rings, and an electron-poor tetramer, **3** (Es_4).

Previous work suggested halogenated solvents would promote a predominantly random conformation[14] while more polar solvents drive a folded structure. If indeed these short tetramers fold in solution, it is well documented that $\pi-\pi$ stacking shifts aryl protons upfield to smaller ppm values.[16] A solvent titration study shown in Figure 2a was conducted at constant temperature and concentration to determine the effects of $\pi-\pi$ stacking as a function of solvent composition for the three tetramers. Each graph represents a solvent titration series for each of the three tetramers at increments of 10 vol % acetonitrile (ACN) in chloroform ($CDCl_3$) from 0% ACN to 100% ACN; all data were referenced to the standard, tetramethylsilane. The ppm shifts for protons a, b, and c of each ring were averaged to represent a single data point per ring at each measured concentration. The original 0% ACN (or 100% $CDCl_3$) value was set to zero to normalize all of the data, and then the change in ppm (Δppm) was plotted as a function of solvent composition.

Δppm, when the solvent is changed from $CDCl_3$ to ACN, indicates a clear upfield shift for the aryl protons of rings 1 and 4 predicted to be involved in $\pi-\pi$ stacking for all three tetramers **1**−**3**.[17] At the same time, the protons expected to experience no $\pi-\pi$ stacking interactions (rings 2 and 3) were observed to remain at $\Delta\text{ppm} \approx 0$ throughout the titration, completely consistent with the expected folded structure. Further, when all three oligomers are compared, the differences in Δppm are also in agreement with expectations. Oligomer **2** is expected to fold better than **1** due to complimentary electrostatics. Rings 1 and 4 of **2** are π-poor and π-rich, respectively, while these two rings in **1** are both π-rich. The electron-poor system of oligomer **3** has the largest Δppm for rings 1 and 4, suggesting closer stacking interactions,[13] although π-poor systems may be more sensitive spectroscopically.[18]

The overall upfield shifting, or Δppm, of the signals corresponding to the protons on rings 1 and 4 in tetramer **1** are relatively small; however, it is clear that the signals from the protons on rings 2 and 3 are not affected by a change in solvent as evidenced in the top graph of Figure 2a. When the data for tetramer **2** are examined (middle graph of Figure 2a), it is again very clear that the signals from the protons on rings 2 and 3 do not shift upfield upon solvent change, indicating no conformational change that moves them to within proximity of a π-stacking event, which is perfectly consistent with the expected helical structure. The data obtained by solvent titration for tetramer **3** (bottom graph of Figure 2a) are even more dramatic. It is clearly evident that the average upfield shifts (Δppm) for the signals corresponding to the protons on rings 1 and 4 are greater than those for the signals corresponding to the protons on rings 2 and 3, which strongly supports a helical folded conformation.

Helical molecular models shown in Figure 2b[19] predict and confirm folded conformations for each tetramer; side chains have been omitted for clarity. The variations in tetramer structures are primarily seen in the slip-stacking angle and distance between rings 1 and 4. A vertical line is shown for each tetramer which is perpendicular to the plane of ring 4 along with a second line extending from the center of ring 4 through the center of ring 1. The angle between these lines helps approximate the slip-stacking offset while the distances between rings are measured through the center of each ring. Exact face to face stacking of the rings would be indicated by an offset angle of 0° and a distance between rings similar to that of constrained and π-stacked benzene rings, or 3.4 Å.[20] Given the conformational constraints of this oPE system, the electronics and/or dipoles of each ring should have an influence on the details of the geometry of the stacked rings,[13] which in turn impacts the folded conformation.[21]

The repulsion that might be expected for the electron-rich rings of tetramer **1** (Et_4, top of Figure 2b) is observed by the 35° slip-stack angle between rings 1 and 4. For tetramers **2** ($EsEt_3$) and **3** (Es_4) the slip-stack angle is approximately 20° and 11°, respectively. These predictions fall directly in line with the data shown in Figure 2a. The angle of slip-stack or offset should directly correlate with the degree of $\pi-\pi$ stacking

(10) Matsuda, K.; Stone, M. T.; Moore, J. S. *J. Am. Chem. Soc.* **2002**, *124*, 11836.
(11) Brunsveld, L.; Prince, R. B.; Meijer, E. W.; Moore, J. S. *Org. Lett.* **2000**, *2*, 1525−1528.
(12) (a) Prince, R. B.; Saven, J. G.; Wolynes, P. G.; Moore, J. S. *J. Am. Chem. Soc.* **1999**, *121*, 3114−3121. (b) Lahiri, S.; Thompson, J. L.; Moore, J. S. *J. Am. Chem. Soc.* **2000**, *122*, 11315-11319. (c) Grubbs, R. H.; Kratz, D. *Chem. Ber.* **1993**, *126*, 149−157. (d) Jones, T. V.; Blatchly, R. A.; Tew, G. N. *Org. Lett.* **2003**, *5*, 3297−3299. (e) Shotwell, S.; Windscheif, P. M.; Smith, M. D.; Bunz, U. H. F. *Org. Lett.* **2004**, *6*, 4151−4154.
(13) Blatchly, R. A.; Tew, G. N. *J. Org. Chem.* **2003**, *68*, 8780−8785.
(14) Hill, D. J.; Moore, J. S. *Proc. Natl. Acad. Sci. U.S.A.* **2002**, *99*, 5053−5057.
(15) Neuhaus, D.; Williamson, M. *The Nuclear Overhauser Effect in Structural and Conformational Analysis*, 2nd ed.; John Wiley & Sons: New York, 2000.
(16) Pickholz, M.; Stafstrom, S. *Chem. Phys.* **2001**, *270*, 245−251.
(17) The average ring chemical shift going from $CDCl_3$ to ACN is +0.05 ppm on the basis of model compounds such as the monomers, dimers, and trimers, which cannot fold.
(18) Ghosh, S.; Ramakrishnan, S. *Macromolecules* **2005**, *38*, 676−686.
(19) Wavefunction-Spartan (molecular mechanics, MMFF minimization).
(20) Lee, M.; Shephard, M. J.; Risser, S. M.; Priyadarshy, S.; Paddon-Row: M. N.; Beratan, D. M. *J. Phys. Chem. A* **2000**, *104*, 7593−7599.
(21) The structures shown in Figure 2b are the minimized conformations; however, it should be noted that the system is dynamic, so this is really only one snapshot.

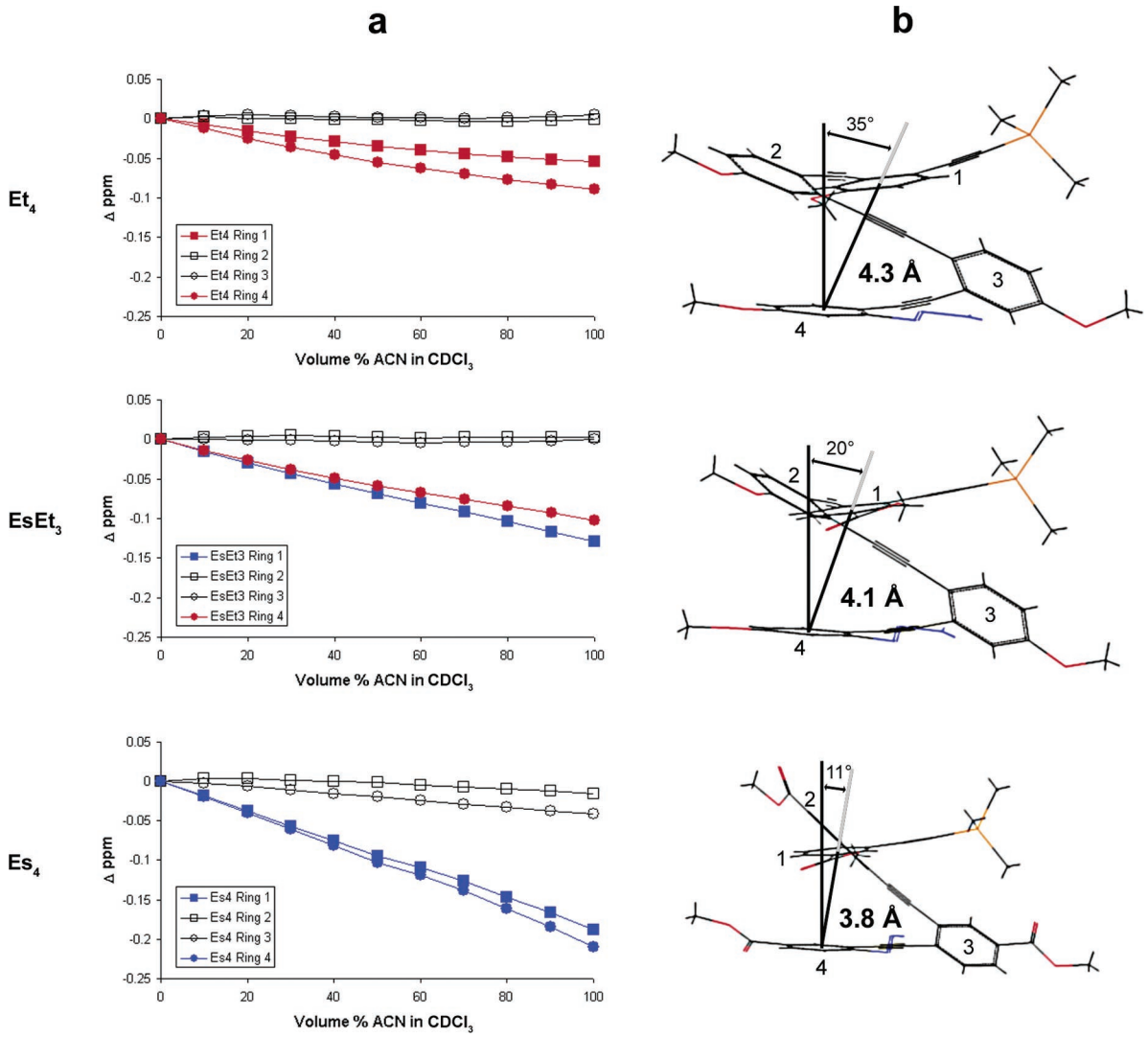

Figure 2. (a) NMR titration curves of **1**−**3** from $CDCl_3$ to ACN. Upfield shifting of rings 1 and 4 is evident, while rings 2 and 3 do not move. Key: (top) **1**, Et_4, (middle) **2**, $EsEt_3$, (bottom) **3**, Es_4. (b) Energy-minimized (MMFF) conformation of tetramers **1**−**3** folded into a helix. The Teg side chains are omitted for clarity. Angles indicate the offset between rings 1 and 4 in the helical conformation. Distances given are between the centers of rings 1 and 4.

experienced by each ring, which would therefore be reflected in the magnitude of upfield shifting experienced by the protons of rings 1 and 4. This is consistent with the observations here in which the system with the smallest angle of offset (**3**, Es_4) is the system in which the largest degree of upfield shifting occurs.

In terms of the distances that can be measured from the center of ring 1 to the center of ring 4, tetramers **1**−**3** are separated by approximately 4.3 Å (Et_4), 4.1 Å ($EsEt_3$), and 3.8 Å (Es_4), respectively. This again provides evidence to support the data obtained in Figure 2a, suggesting that protons of tetramer **3** (Es_4) are most affected in the helical conformation. In addition, the tilt, or face-to-edge stacking, between rings 1 and 4 is very small. The models show a trend in which this small tilt is observed to increase from tetramer **3** to tetramer **1**. Table 1 summarizes the ring proton shifts (Δppm) for the end points of the titrations of tetramers **1**−**3** and shows that in all cases rings 1 and 4 shift upfield while rings 2 and 3 move very little, which is perfectly consistent with the expected helical structure.

By examining the 1D NMR traces of all the aromatic protons (Figure 3a) and coupling these observations with the molecular models of tetramers **1**−**3** (Figure 3b), more details regarding the ppm shifting of each aryl proton can be found. Ring

Table 1. Average Δppm ($CDCl_3$−ACN) Shifts for Aryl Protons for **1**−**3**

ring no.	**1** (Et_4)	**2** ($EsEt_3$)	**3** (Es_4)
1	−0.09	−0.13	−0.21
2	0.01	0.00	−0.04
3	0.02	0.00	−0.02
4	−0.05	−0.10	−0.19

assignments were made using a combination of *J*-coupled correlation spectroscopy (COSY) and heteronuclear multiple-bond correlation (HMBC) NMR experiments to identify which protons are attached to each ring of the tetramers. For tetramer **1**, the model shown at the top of Figure 3b suggests that protons 1a, 4a, and 4b would experience the largest change in chemical environment. The NMR spectra shown alongside the model in Figure 3a (top) support this observation as these three protons experience the largest change from $CDCl_3$ to ACN. Proton 4b is influenced by the aromatic ring, while protons 1a and 4a are influenced by the triazene and acetylene functionalities, respectively. At the same time, very little upfield shift is observed for proton 4c, while proton 1c actually shifts *downfield*. In general, we observe this small downfield shift for the aromatic protons

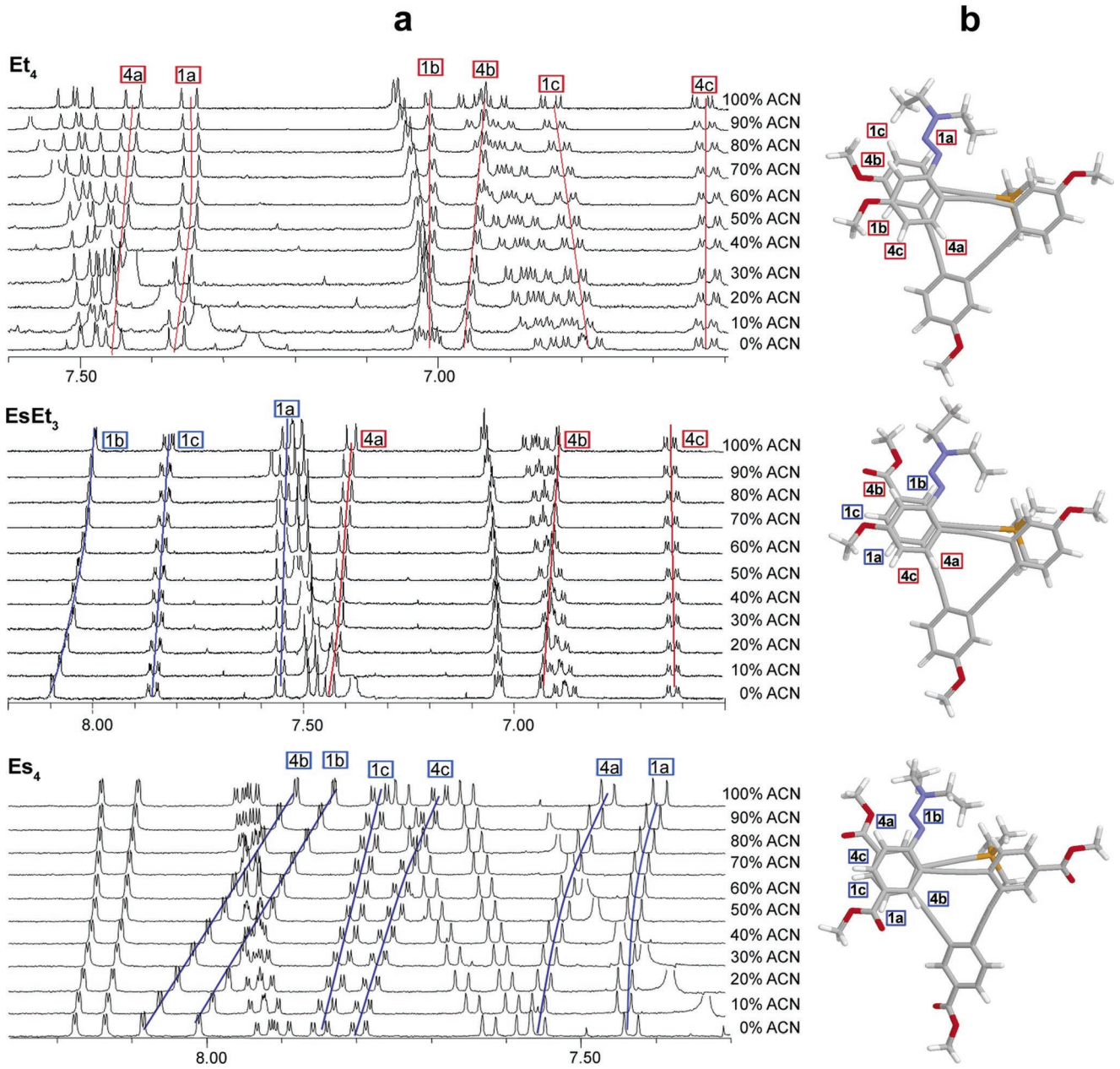

Figure 3. (a) NMR traces for each concentration of ACN in $CDCl_3$ for tetramers **1**−**3** (1.25 mM, 400 MHz, 298 K). Individual signals from rings 1 and 4 have been labeled and were assigned by a combination of COSY and HMBC 2D NMR experiments. Tetramethylsilane was used as the reference: (top) **1**, Et_4, (middle) **2**, $EsEt_3$, (bottom) **3**, Es_4. (b) Top down views of molecular models.

of model compounds which is most likely due to the change in dielectric constant of the solvent.[12b,17] The standard tetramethylsilane corrects this shift. At the same time, the inherent downfield shifting of the protons going from $CDCl_3$ to ACN[17] provides further support that $\pi-\pi$ stacking of rings 1 and 4 cause the upfield shifts we observe in ACN. The overall upfield shifts for **1** are the smallest of the three tetramers, again indicating a very weak interaction between rings 1 and 4 overall.

For tetramer **2** ($EsEt_3$) the model indicates that the protons of rings 1 and 4 that should be most affected by the folded conformation are 1b, 1c, 4a, and 4b. Proton 1b is located under the triazene group, proton 1c is influenced by the ester function, proton 4a is located near the acetylene bond, and proton 4b is located above ring 1. Interestingly, protons 1b and 4c of tetramer **1** as well as protons 1a and 4c of tetramer **2** do not experience significant upfield shift. These protons, although labeled differently due to chemical connectivity, are found in the same locations on the two foldamers (see Figure 3b, top and middle). The molecular model of tetramer **3** (Es_4) indicates that the rings are nearly on top of one another, suggesting that all of the protons on rings 1 and 4 should be affected and all their signals should shift upfield accordingly. Indeed, this is what is observed in the NMR spectra at the bottom of Figure 3a. In fact, all of the proton signals associated with rings 1 and 4 shift upfield considerably more than those of tetramer **1** or **2**.

In addition to the 1D data, we speculated that the terminal TMS (trimethylsilane) group would provide an excellent NMR probe in NOESY experiments for two main reasons. The chemical shift of the TMS falls at a unique region in the spectra (~0.2 ppm) compared to those of the rest of the protons in the molecule, and the methyl groups extend beyond the aromatic backbone plane by ~2.0 Å. Due to the inherent distance

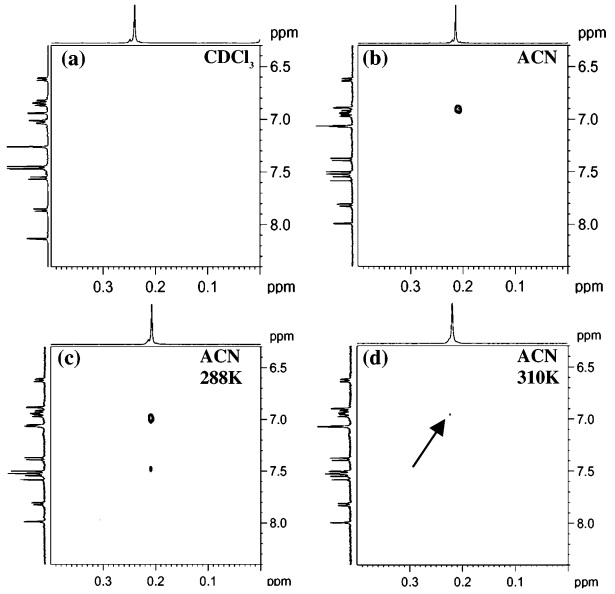

Figure 4. Partial NOESY spectra of **2**, $EsEt_3$ (1.25 mM, 400 MHz, 299 K, mixing time 0.1 s), for the TMS and aryl regions in $CDCl_3$ (a) and ACN (b). No cross-peak is observed in $CDCl_3$, while a strong NOE is present in ACN. Partial NOESY spectra of **2** (1.25 mM, 400 MHz, mixing time 0.1 s) in ACN revealing the TMS to aryl interaction at 288 K (c) and 310 K (d).

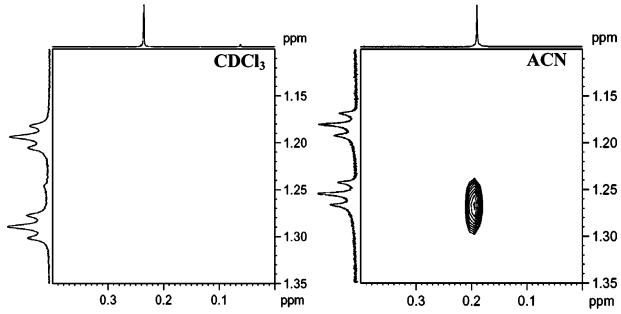

Figure 5. Partial ROESY spectra of **3**, Es_4 (1.25 mM, 600 MHz, 298 K, mixing time 0.3 s), for the TMS and triazene regions in $CDCl_3$ (left) and ACN (right). No cross-peak is observed in $CDCl_3$, while a strong NOE is present in ACN.

dependence of NOESY, which is typically 4−5 Å,[15] and the likelihood of similar stacking distances, this additional ∼2.0 Å plays an important role.

Tetramer **2**, $EsEt_3$, was examined by 2D (NOESY) ^{1}H NMR studies at room temperature in $CDCl_3$ and ACN (Figures 4a and 4b). The TMS peak appears at 0.2 ppm, and the aryl peaks corresponding to ring 3 appear at 7.51 ppm (3a), 7.07 ppm (3b), and 6.96 ppm (3c) in ACN. A strong NOE between the TMS protons and proton 3c was observed in ACN but is completely absent in $CDCl_3$ as shown by the partial NOESY spectra in Figures 4a and 4b. The NOE interactions are consistent with a folded structure in which the electron-poor ring 1 stacks with the electron-rich ring 4 (see Figure 3b, middle).

When tetramer **3** was examined by 2D (ROESY) ^{1}H NMR studies (Figure 5) at room temperature in $CDCl_3$ and ACN, a strong NOE cross-peak was observed between the terminal TMS of the molecule and a methyl from the triazene end group of ring 4 *only* in ACN. This cross-peak is completely absent in $CDCl_3$, indicating tetramer **3**, Es_4, folds in ACN but not in $CDCl_3$. This NOE further indicates the TMS group continues in the progression of the helix, consistent with the NOE observed for **2** in Figure 4b, and that rings 1 and 4 are closer to face-to-face stacking than face-to-edge stacking since face-to-edge stacking would most likely move the two end groups (triazene and TMS) away from each other. Extracting distance data based on the integrals of the NOESY/ROESY cross-peaks (see Table 2) confirms the close proximity of the TMS and ring 3 (**2**, $EsEt_3$) or the TMS and triazene end groups (**3**, Es_4).[22] At room temperature, the TMS is ca. 2.29 Å away from proton 3c of **2** and the triazene is ca. 3.36 Å from the TMS of **3**.

Table 2. Calculated NOESY Distances

molecule	TMS to X[a] distance (Å)
2 ($EsEt_3$)	2.29
3 (Es_4)	3.36

[a] X = proton 3c for **2** and a methyl of triazene for **3**.

When tetramer **1** was examined by NOESY, no NOE signal was observed. The lack of NOE peaks for tetramer **1** is most likely due to the presence of the two electron-rich rings which are not expected to promote folding as strongly and/or force the two rings (1 and 4) further apart due to the higher electron density, which consequently pushes the TMS protons out of the NOE distance correlation range (4−5 Å). The 1D proton chemical shift values discussed in Figures 2 and 3 support folding of this oligomer, but are also consistent with the lack of NOE cross-peaks since the Δppm is the smallest of all three oligomers and the distance (measured by modeling) is the largest.

Other NOESY studies on folding oligomers[4] have indicated that low temperature is required to obtain an NOE cross-peak. All of the work presented thus far was collected at room temperature. Taking into account this possible temperature dependence, we performed a limited temperature study to determine whether the NOE signals we observed for tetramer **2** were temperature dependent. Upon cooling of tetramer **2**, $EsEt_3$, to 288 K, a new NOE signal appears between the TMS protons and proton 3a so that two NOEs are present (Figure 4c). These signals correspond to distances of 2.42 and 2.97 Å, respectively, for protons 3c and 3a. Conversely, when the temperature is increased to 310 K (Figure 4d), the NOE for proton 3a completely disappears and the original proton 3c NOE is diminished by 95%. This temperature variation in NOE is consistent with a folding pathway in which rings 1 and 4 would interact more strongly with one another as the temperature is reduced, leading to the additional NOE signal. Conversely, elevating the temperature reverses this effect, resulting in the observed decrease in the two NOE signals and intensities. A 1D study of tetramers **2** and **3** (Figure 6) over the same temperature range reveals the expected downfield shift of the aromatic protons on rings 1 and 4 with increasing temperature and tetramer **3** shifts more than tetramer **2**. The larger observed shifts for the protons of tetramer **3** are likely due to the fact that **3** is stacked

(22) As the distance between protons a and c on one ring can be approximated as 2.44 Å, a relation between the integration of the observed cross-peaks and the distances can be determined (see the Supporting Information for more details).

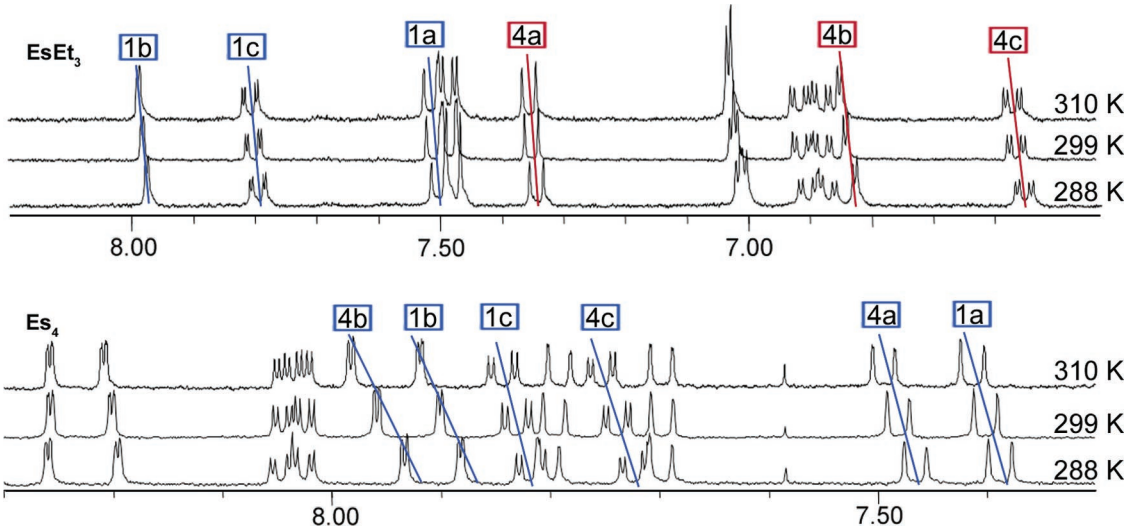

Figure 6. NMR traces in ACN for tetramers **2**, $EsEt_3$ (top), and **3**, Es_4 (bottom), at 288, 299, and 310 K. Downfield shifting is evident as temperature is increased. Tetramethylsilane was used to reference each spectrum. Individual signals from rings 1 and 4 have been labeled and were assigned by a combination of COSY and HMBC 2D NMR experiments.

more closely than **2**. This is consistent with the data discussed above. In addition, since **3** is more closely packed, a small change in distance would influence the Δppm more. Another intriguing possibility is that **2** is more stable due to complimentary electrostatics. Iverson[3] showed that complementary π-systems (π-rich and π-poor) associated more than two π-poor systems by 1 order of magnitude. His study formed a charge-transfer complex, unlike ours; however, the trend is similar. Currently, we cannot distinguish these two possibilities, although the first one in which **3** packs more tightly is most consistent with the data presented. What is clear is that the observations in the 1D spectra (Figure 6) agree with the NOE variable-temperature data.

When the TMS region for Figures 4 and 5 is examined closely, it is evident that the signal for the TMS protons also shifts upfield in ACN. The TMS end group of tetramer **3** (Es_4) is most affected, shifting upfield 0.06 ppm. The magnitude of shifting, although small, is directly related to the tetramer studied and shows a larger shift going from **1** to **3**. This is additional support that the TMS end group lies over the plane of ring 3.[23]

(23) Table S1 in the Supporting Information provides specific data for this calculation.

Conclusions

Very short novel oPE oligomers are reported and shown to fold at room temperature by 1D and 2D NMR. NOESY provides the first high-resolution data on solvent-driven PE oligomers and confirms oPE as a versatile and suitable scaffold to construct foldamers. Tetramers **2** and **3** appear to fold best with the potential to unfold at higher temperature, indicating an additional route for denaturation. Additional studies to determine the structure most suitable for stable helix formation with the oPE systems is required. The 1D chemical shifts appear to be more sensitive to aromatic stacking than NOE interactions. oPE oligomers will generate high aspect ratio objects when folded and are being studied for self-assembly into larger, tertiary-like structures as well as for the display of chemical functions in 3D space.

Acknowledgment. We thank L. Charles Dickinson for NMR assistance. T.V.J. thanks the Ford Foundation for financial support. G.N.T. thanks the NSF-CAREER Award for funding. We thank Prof. Rich A. Blatchly for many helpful discussions.

Supporting Information Available: Complete synthetic procedures for preparation of oligomers **1**−**3**. This material is available free of charge via the Internet at http://pubs.acs.org.

JA053530+